Assessing Use of the Excess Shear Stress Equation to Estimate Cohesive Bank Erosion Rates Under Different Stream Channel Characteristics

Justin Condon, Project Engineer, S&ME, Inc., Knoxville, Tennessee; and the University of Tennessee, Knoxville, Tennessee, jcondon4@outlook.com
John S. Schwartz, Professor and Director of the Tennessee Water Resources Research Center, University of Tennessee, Knoxville, Tennessee, jschwart@utk.edu

Abstract

Stream bank erosion rates are commonly estimated using the excess shear stress equation, however the equation appears to overestimate annual bank retreat where previous studies have suggested a modidifed equation with an 'α' coefficient to adjust for multiple factors affecting applied hydraulic shear stresses (τ); the modifed equation becomes: $\varepsilon_r = k_d\,(\alpha\cdot\tau - \tau_c)$. The objective of this study was to determine whether the excess shear stress equation overestimates annual bank retreat, and whether the modified equation with an α coefficient can effectively be applied to more accurately estimate bank retreat from fluvial erosion. The study included seven stream bank sites on Beaver, Bullrun, and Stock creeks located in East Tennessee with all streams having USGS gaging stations located downstream. Bank erosion pins were placed at four channel morphology/vegetation classes to measure retreat (ε_r) over a one-year period; they were straight and curved channels with and without vegetation. Steel erosion pins 46 cm in length were installed vertically along the lower, middle, and upper bank positions. A mini-jet device was used to approximate the soil erodibility coefficient (k_d) and critical shear stress (τ_c) at each site. Flow stage were modeled using HEC-RAS to determine τ at each pin. Results for annual bank retreat for straight channel with vegetation ranged from -0.91 to -4.57 cm, straight channels without vegetation ranged from -2.13 to -14.63 cm, outside bends of curved channels with vegetation ranged from -1.52 to -8.53 cm, and outside bends of curved channels without vegetation ranged from -17.37 to -23.77 cm. Bank retreat rates were substantially reduced with vegetation. Per channel morphology/vegetation class, α coefficients averaged 0.3467, 0.2677, 0.2504, and 0.3100 for straight channels with and without vegetation and curved channels with and without vegetation, respectively. Class differences were significantly different for straight channels vegetated and non-vegetated, and non-vegetated straight and curved channels ($p < 0.05$). All α coefficients were indicating the excess shear stress equation overpredicted annual bank retreat, though α varied widely due to multiple factors. Further research is needed to improve the use of this equation to predict bank retreat under different channel conditions.

Introduction

Excessive stream bank erosion is a major problem nationally degrading water quality and aquatic ecosystems, and compromising agricultural lands and urban infrastructure. Siltation, or the excessive fine sediment consisting of sand, silt, and clay in stream channels is the leading cause of water quality impairment in the United States (Waters 1995; USEPA 2000, 2006; Govenor et al. 2017). It can cause ecosystem level impacts to fish, macroinvertebrates, and other aquatic organisms (Wood and Armitage 1997; Henley et al. 2000; Schwartz et al. 2011). With fish, prolonged periods of elevated suspended sediment can cause mortality; depress growth, reproduction, and recruitment; shift predator–prey relationships; and elicit avoidance behavior migrating from impacted reaches (Newcombe and Jensen 1996; DeRobertis et al. 2003). Sources of fine sediment in streams generally are from watershed disturbances such as channelization and poor agricultural practices. In urban watersheds, sediment sources in runoff can be from developments without adequate stormwater control measures, and also from bank erosion and channel incision caused by hydromodification (Bledsoe and Watson 2001; Schilling et al. 2011; Anim et al. 2018). Bank erosion can be the dominant source of instream fine sediment contributing up to 60-80% of the total sediment loads as reported by Simon and Rinaldi (2006). Percent contributions of instream sediment from bank erosion have been similarly reported by others though it varies depending on physiographic region, watershed characterizes, and land use practices (Simon 1995; Green et al. 1999; Simon and Klimetz 2008; Kronvang et al. 2013; Palmer et al. 2014). Elevated suspended sediment loads in streams generally occur in geomorphologically unstable channels (Simon et al. 2004). With siltation as a leading cause for water quality impairment and lotic ecological degradation, there is a need for improved restoration measures through watershed planning and management to lessen impacts from this stressor (Shields et al. 1995; Schwartz et al. 2008; Violin et al. 2011).

Improving watershed restoration plans to reduce instream fine sediment from bank erosion requires advancements in field assessment methods and models to better predict excessive erosion rates, rates beyond which should occur naturally. Improvements to field assessment methods and models quantifying bank stability and erosion rates need to apply geomorphic-geotechnical processes (Thorne and Tovey 1981; Simon and Darby 1999; Simon and Thomas 2002; Chen and Duan 2005; Curran and Hession 2013). Bank erosion rates can be predicted through various means from empirical to process-based approaches (Klavon et al. 2017; Saadon et al. 2021). An empirical approach, the Bank Assessment for Non-point Source Consequences of Sediment (BANCS) uses two indexes, the Bank Erosion Hazard Index (BEHI) and the Near Bank Stress Index (NBS) (Rosgen, 1996, 2006). The BEHI is a rapid field assessment used to approximate the vulnerability of a bank for excessive erosion, while the NBS index qualitatively estimates the erosive force on the bank during bankfull flows (Allmanová et al. 2019). A process-based assessment approach, the Rapid Geomorphic Assessment (RGA) applies nine field metrics to quantify stable and unstable channels, and it is based on channel evolution model concepts (Darby and Thorne 1995; Simons and Downs 1995; Simon and Klimetz 2008; Davis and Harden 2014; Booth and Fischenich 2015). Differing from BANCS, the RGA is a reach-scale assessment that includes channel adjustment metrics accounting for vertical downcutting and lateral bank erosion. The Bank Stability and Toe Erosion Model (BSTEM) and the Conservational Channel Evolution Pollutant and Transport System (CONCEPTS) are process-based models (Langendoen 2000; Simon et al. 2000). BSTEM applies both fluvial erosion and mass wasting processes to estimate a factor of safety for bank stability. The CONCEPTS model applies the same processes but dynamically accounts for sediment fluxes from bank retreat and stream transport.

Bank erosion models, such as BSTEM and CONCEPTS rely on the excess shear stress equation to estimate cohesive-soil bank retreat from fluvial erosion (Langendoen 2000; Simon et al. 2000). Bank erosion rates (ε_r) by the excess shear stress equation is as follow: $\varepsilon_r = k_d\ (\tau - \tau_c)^m$; where k_d is the erodibility coefficient ($m^3/N \cdot s$), τ is the applied hydraulic shear stress (Pa) at the bank boundary, τ_c is the critical shear stress (Pa) for bank soil erosion, and 'm' is a coefficient assumed to be unity (Hanson 1990a; Hanson and Cook 2004). Computed values for ε_r are typically converted to units of cm/s. Reflecting physical resistance to erosion, the parameters k_d and τ_c are soil properties, whereas τ is the stream hydraulic force that may cause erosion. Several methods have been used to measure k_d and τ_c including a laboratory hole erosion device (Wan and Fell 2004); flumes (Briaud et al. 2001; Mahalder et al. 2022), and the jet test device (Hanson 1990b; Hanson and Simon 2001; Clark and Wynn 2007; Al-Madhhachi et al. 2013; Daly et al. 2013; Mahalder et al. 2018). The jet test device has been widely used, and Simon et al. (2010)

introduced a mini-version of this device. Estimates for k_d and τ_c can vary widely due to many factors including different approaches for field measurement and data analysis, bank spatial variability of soil physical and geochemical properties, and bank soil moisture, subaerial processes, and root density (Wynn and Mostaghimi 2006; Wynn et al. 2008; Mostafa et al. 2008; Midgley et al. 2012; Daly et al. 2015a&b; Mahalder et al. 2017; Khanal et al. 2020). Knowledge of the potential factors affecting for k_d and τ_c supports with obtaining relevant estimates of local soil resistance properties.

In addition to the variability associated with bank soil properties and measurements of k_d and τ_c, τ is influenced by channel planform and boundary conditions (Duan 2005; Yu et al. 2015). Estimates for τ are commonly computed using a reach-scale equation derived from a momentum balance as: $\tau = \gamma \cdot R \cdot S$, where γ is the specific weight of water, R is the reach-average hydraulic radius, and S is the energy slope (Sturm 2021). Although this equation is typically used to obtain a reach-scale τ, shear stresses are not uniformly distributed along a channel's boundary. Accelerated and decelerated flows from changes in channel morphology and deflected flows from instream structures govern τ locally varying fluvial erosion rates along a channel's banks. The distribution of τ varies along a channel is a function of its planform geometry, i.e., straight, meander, and braided channels. In meandering channels, accelerated flows occur on the convex side of the bend and secondary currents on the concave side (Dietrich 1987, Ferguson et al. 2003; Chen and Duan 2005). A local maximum bed τ occurs at the pool exit. Large roughness elements can cause accelerated flows or jets directed into banks, commonly consisting of woody debris and/or log jams (Manner et al. 2007; Addy and Wilkinson 2019; Ismail et al. 2021). Bank vegetation interactively influences both τ_c and τ where increased bank vegetation infers greater root density in the soil matrix thus increasing τ_c (Wynn 2004; Curran and Hession 2013; Smith et al. 2021). Whereas, greater density of bank vegetation reduces τ at the reach-scale and locally on a bank from increased flow resistance (Kean and Smith 2004; Hopkinson and Wynn-Thompson 2016; Termini 2016).

With multiple factors affecting local boundary hydraulic forces and bank heterogeneous physical properties, parameters in the excess shear stress equation (τ, k_d, and τ_c) need to account for these factors. Under different channel conditions, the use of this stress equation may underpredict or overpredict actual bank erosion rates. Using BSTEM, Midgely et al. (2014) found erosion rates were underestimated apparently due to a composite bank structure with a stratified gravel layer. Using HEC-RAS with BSTEM, Mahalder (2018) found bank retreat was overestimated at several cohesive soil bank locations in West Tennessee with long-term measurements of channel geometry. Modifications to the excess shear stress equation has been suggested to account for these factors (Langendoen and Simon, 2008, 2009; Daly et al., 2015b). Accounting for complex channel hydraulics and near-bank turbulence from vegetation and instream structures, τ in the equation can be adjusted with a coefficient, defined here within as 'α'. The modified equation becomes: $\varepsilon_r = k_d \cdot (\alpha \cdot \tau - \tau_c)$.

In order to estimate α, for different channel conditions through experimentation, bank erosion (ε_r) must be known as well as the equation independent variables. Long-term estimates for ε_r can be obtained in the field by various means (Lawler 1993). Common approaches to measuring ε_r include repeated surveyed cross-sections with fixed datums, and the use of erosion pins. Other more advanced methods include photo-electronic erosion pins (PEEPs) and terrestrial laser scanners (Lawler 2008; Myers et al. .2019). Though many studies have used these various methods to measure bank retreat (Addul-Kadir and Ariffin 2012; Kronvang et al. 2013; Pope and Odhiambo 2013), studies have not merged ε_r with concurrently collected field measured of τ, k_d, and τ_c. To measure τ, continuous stage and discharge measurements are needed. Through a coordinated field study an α value can obtained in the above modified shear stress equation.

The objective of this study was to assess whether the excess stream stress equation tends to overpredict annual estimates of bank treat on cohesive stream banks, and whether this equation can be parameterized with an α·coefficient to provide more accurately estimates of annual bank retreat, accounting for the effects of morphology and vegetation. Because many factors can influence prediction of bank erosion rates, this studied focused on τ and influences on the channel hydraulics associated with planform curvature (straight or meandering), and bank vegetation resistance (bare soil or vegetated). This study was unique in that it combines the use of erosion pins for measuring bank retreat over time, HEC-RAS modeling to determine τ based on different flow stages in relation to vertical pin position, use of USGS gaging stations to determine flow durations in contact with deployed pins, and the use of the jet test device to measure soil erodibility parameters. A secondary objective was to assess qualitatively the measurement variability to better understand driving forces in bank retreat processes.

Methods

Study Area

Beaver, Bullrun, and Stock creek watersheds are located within Anderson, Knox, and Union counties of East Tennessee (Figure 1). Study sites in these streams were chosen because cohesive soil banks were actively eroding and a USGS gaging station was located downstream. Eight sites were chosen within these watersheds varying in drainage area between 5.7 to 100.4 km² (Table 1). Watershed land uses differed in composition including forest, pasture, and urban developed. East Tennessee is in the humid subtropical climate type, with annual average precipitation reported as 132 cm and an average temperature range of -0.6°C to 31.1°C with lows below -8°C and highs near 38°C in recent years (NOAA 2022).

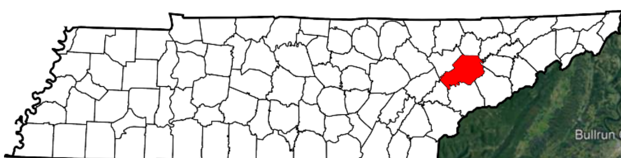

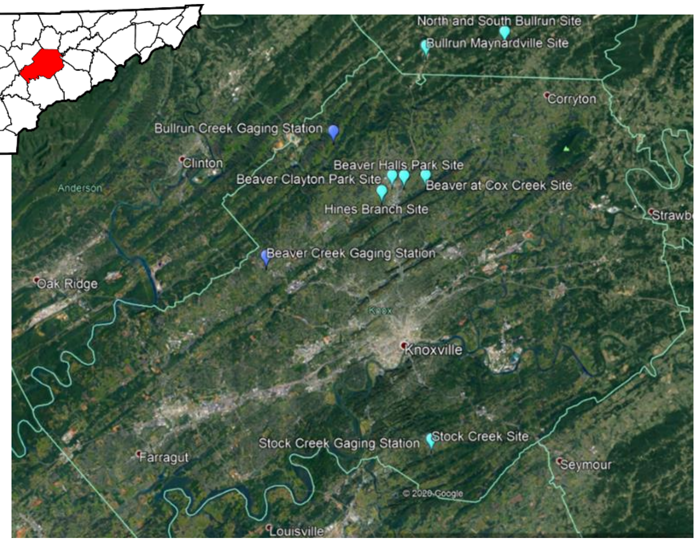

Figure 1. Map showing location of study area in East Tennessee and the monitoring sites within Beaver, Bullrun, and Stock creek watersheds.

Study Design

As noted above, study sites were selected so that continuous flow data were available from USGS gauging stations during the study period. USGS gauging station numbers were: Stock Creek (034991109); Bullrun Creek (03535000), and Beaver Creek (03535200). Each site was installed with multiple erosion pin placements, differing among four channel morphology/bank vegetation classes. The classes were: 1) straight channel with bank vegetation, 2) straight channel with no bank vegetation, 3) channel curvature with bank vegetation, and 4) channel with no bank vegetation (Table 1). Bank vegetation consisted of woody plants and dense root structures, and riparian tree canopy. Channel curvature generally consisted of meander bends though selection was made based on flow directed to the concave side on any channel curvature. The erosion pins were installed between March 22, 2019 and June 14, 2019, and monitoring terminated May 2020. Erosion pin exposure (ε_r) was measured between September and December of 2019, and again in May 2020 for a total period of about one-year. Parameters k_d, and τ_c. were measured by use of a mini-jet test device. Estimates for τ duration was the time period pins were exposed to a high-flow event and the computed reach-scale τ for that flow stage (Condon 2020). Details are described below.

Table 1. Study sites locations and drainage area, and monitoring information on number of erosion pins, dates installed, and channel class (1 = straight channel with bank vegetation, 2 = straight channel with no bank vegetation, 3 = outside bend with bank vegetation, and 4= outside bend with no bank vegetation).

Site	Latitude	Longitude	Drainage Area (km^2)	Number Pins	Date Pins Installed	Channel Class
Stock Creek	35°52'42"N	83°53'43"W	36.6	20	6/14/2019	1,2
Bullrun Maynardville	36°10'48"N	83°54'01"W	110.4	12	6/14/2019	1
South Bullrun	36°11'28"N	83°49'31"W	48.5	12	6/14/2019	2,3
North Bullrun	36°11'28"N	83°49'31"W	32.0	6	6/14/2019	2
Hines Branch	36°04'06"N	83°56'32"W	5.7	12	4/30/2019	1,3,4
Beaver Clayton Park	36°04'49"N	83°55'57"W	59.3	12	4/30/2019	1,2
Beaver Halls Park	36°04'40"N	83°55'16"W	39.1	24	4/30/2019	2,3,4
Beaver at Cox Creek	36°04'50"N	83°54'02"W	36.1	29	3/22/2019	1,2,3,4

Stream Bank Field Measurements

Erosion pins were installed and monitored according to Lawler (1993), and used to obtain annual values for ε_r. Steel rebar pins were 1.3 cm diameter with an approximate length of 46 cm. Erosion pins were hammered into the bank normal to the bank slope in sets of three in the vertical at the upper, middle, and lower bank locations. The lower pin was placed near the baseflow water surface stage. Approximately 0.2 cm of the erosion pins were left exposed when placed in the banks. Pin exposures were measured to the nearest 2.5 mm using a fiberglass measuring tape. During site inspections if a pin was unable to be found, the surrounding bank and other pins were examined to determine if the pin was buried signifying deposition, or if the pin was lost signifying erosion occurred > 40-45 cm. Erosion and deposition were calculated by taking the finite difference between the initial and final measurements over the monitoring period. Erosion was denoted as negative values whereas deposition was denoted as positive values. A total of 127 pins produced acceptable data, and the distribution of these pins per the four channel classes is summarized in Table 2.

Table 2. Summary of the number of pins installed per channel morphology/vegetation class. A total of 127 pins were monitored throughout a one-year study period in 2019-2020.

Channel Morphology/ Vegetation Classes	**Straight with bank vegetation**	**Straight with no bank vegetation**	**Curved with bank vegetation**	**Curved with no bank vegetation**
Class Designation Number	1	2	3	4
Number of Pins	44	29	36	18
Percent of Pins per Class	35	23	28	14

The mini-jet device was used at each site to estimate k_d, and τ_c. applying standard field and analysis methodology (Hanson and Simon 2001; Hanson and Cook 2004; Simon et al. 2010; Al-Madhhachi et al. 2013). Six jet tests were completed at each site, and two each at the lower, middle, and upper bank locations. Test sites were located on exposed cohesive soil with no roots, rocks, or vegetation on the bank surface, and conducted when banks were acceptably moist. An 1/6 horsepower submersible pump powered by a 1000-Watt Yamaha EF1000iS portable generator was used to deliver water from the stream to the jet device. Single pressures between 35 and 48 kPa (5-7 psi) were generated at the device nozzle depending on the bank vertical position. The time interval used to measure scour hole depth started at one-minute intervals followed by two-minute intervals until there was three consistent depth readings. Scour depth interval data were analyzed using Blaisdell method to compute k_d, and τ_c, utilizing a spreadsheet developed by Daly et al. (2013).

Stream Hydraulic Shear Stress Estimates

Fluvial erosion at pins were dependent on a time series of τ, where τ is a function of flow stage and discharge. Estimates for reach-scale bed τ were computed by: $\tau = \gamma \cdot R \cdot S$ with variables defined in the Introduction. Hydraulic radius (R) and slope (S) are a function of channel cross-sectional geometry and discharge. The HEC-RAS 5.0.7 1D steady flow models were used to obtain τ at different flow stages per site. Channel cross-sections were surveyed at all pin locations, and upstream and downstream for use in the model. Continuous discharge records were obtained from USGS gauging stations located downstream of the erosion pin sites. Because the pin locations were not at the USGS gaging stations but upstream in the watershed, flow records at the pin locations required to be adjusted from the USGS gaging stations.

Continuous flow records for each pin site was generated by the use of the upstream USGS gagging station and regression relationships based on flow statistics between the USGS gaging station and the pin site (Condon 2020). USGS StreamStats was used to obtain 13 flow duration statistics ranging from 10 to 99.5 percent duration exceedances at the USGS gaging station and the erosion pin site. A linear regression equation was developed from these flow statistics with the pin site as the dependent variable (y) and the USGS gaging station as the independent variable (x). Each pin site with its unique regression equation was applied to the USGS continuous flow data to compute a flow time series at the pin site. Flow time series were inspected over a discharge range, and selected discharges were modeled with HEC-RAS to obtain flow depths, τ, and the period of time each pin were subjected to erosive flow.

As a check on the regression relationships adjusting the discharge time series at the different study sites, a field measurement of discharge was completed during base flow in May 2020. The standard USGS area-velocity method was used to compute discharges for surveyed cross-sections measuring water depths and velocities along sub-sections. Velocities were measured using a Marsh-McBirney Flo-Mate 2000 current meter. Field estimated discharges were compared with the computed discharges from the regression relationships (as described above). All site comparisons of these two discharges estimates were within 0.17 m^3/s of each other.

Modified Excess Shear Stress Equation

Dimensionless α coefficients for the modified excess shear stress equation were estimated for the four channel classes (Table 2) with measured and computed values for ε_r, k_d, τ_c, and τ. The modified equation becomes: $\alpha = (\varepsilon_r/k_d, + \tau_c)/\tau$. As noted above, k_d ($m^3/N \cdot s$) and τ_c (Pa) were obtained from the mini-jet device, and measures averaged per pin site Estimates for ε_r (m) was computed by retreat depth into the bank measured over the study period, divided by the time the pin was exposed to flow (seconds) and an average τ (Pa) for three flow stages reflecting the three vertical pin positions (Figure 2). Average τ were obtained from the HEC-RAS model. If $\tau > \tau_c$ for an event flow stage, then the event average τ for a pin was computed based on equations summarized in Table 3. These equations apply the Bagnold (1960) formula where τ is linearly proportional with τ at the water surface as zero and τ at the bed as maximum (Figure 2).

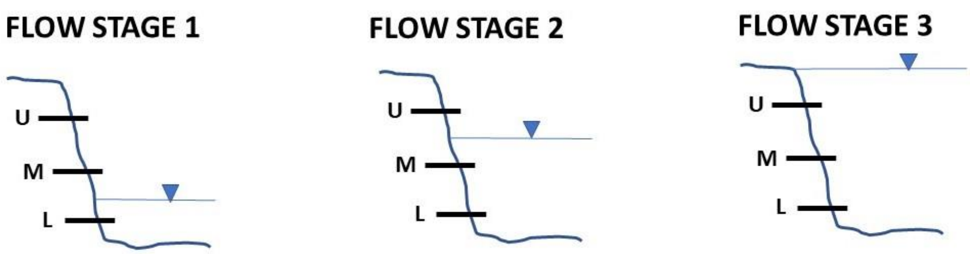

$\tau_{1U} = 0$
$\tau_{1M} = 0$
$\tau_{1L} = \gamma \cdot R_1 \cdot S_1$

$\tau_{2U} = 0$
$\tau_{2M} = 0.2 \cdot \gamma \cdot R_2 \cdot S_2$
$\tau_{2L} = \gamma \cdot R_2 \cdot S_2$

$\tau_{3U} = 0.2 \cdot \gamma \cdot R_3 \cdot S_3$
$\tau_{3M} = 0.5 \cdot \gamma \cdot R_3 \cdot S_3$
$\tau_{3L} = \gamma \cdot R_3 \cdot S_3$

Figure 2. Bank profile schematic showing vertical pin positions (U = upper, M = mid, and L = lower) for three flow stages and the corresponding equations to estimate τ. Equations are denoted as: τ_{ij}, with i = flow stage (1,2, and 3), and j = pin position (U, M, and L).

Table 3. Time-weighted estimates for average τ based on pin position and event flow stage as shown in Figure 2 (T_{ij} = time pin exposed for flow at stage i at pin j).

Pin	Bank Retreat (ε_r)	Time-weighted Average τ Equations
U	Pin U bank retreat (m) /total time (s) at Flow Stage 3	$\tau_{(U)} = \tau_{3U}$
M	Pin M bank retreat (m) / total time (s) at Flow Stages 2 & 3	$\tau_{(M)} = (\tau_{2M} \cdot T_{2M} + \tau_{3M} \cdot T_{3M}) / (T_{2M} + T_{3M})$
L	Pin L bank retreat (m) /total time (s) at Flow Stages 1, 2, & 3	$\tau_{(L)} = (\tau_{1L} \cdot T_{1L} + \tau_{2L} \cdot T_{2L} + \tau_{3L} \cdot T_{3L}) / (T_{1L} + T_{2L} + T_{3L})$

Results and Discussion

Measured Erodibility Parameters

The mini-jet device was used to estimate τ_c and k_d for each study reach which may have had multiple vertical pin sites. Field tests were conducted between September 15, 2019 and December 1, 2019; and summarized in Table 4 for each study reach. Erodibility parameters for two lower bank tests were averaged, and due to the variability the four middle and upper bank tests were averaged. These averaged values as reported in Table 4 were used the parameters used in modified excess shear stress equation. Averaged τ_c and k_d values were variable, ranging between 0.03 and 6.87 Pa, and 0.66 and 18.99 $cm^3/N \cdot s$, respectively. Though the erodibility parameter measurements were highly variable, this variability was similarly reported by others (Daly et al. 2015a; Mahalder et al. (2018). Mahalder et al. (2018) measured τ_c and k_d in the Ridge and Valley Province in East Tennessee and reported similar ranges.

Table 4. Erodibility parameters (τ_c and k_d) measured at seven study reaches for lower and mid/upper bank positions.

Bank Pin Position	Bullrun Maynard-ville	South/ North Bullrun	Hines Branch	Beaver Clayton Park	Beaver Halls Park	Beaver at Cox Creek	Stock Creek
Low							
τ_c (Pa)	5.93	0.03	0.70	0.07	1.06	2.77	0.29
k_d ($cm^3/N \cdot s$)	0.66	2.88	3.44	1.98	2.67	3.76	9.58
Mid/Upper							
τ_c (Pa)	6.87	0.06	2.21	2.01	2.48	4.29	6.45
k_d ($cm^3/N \cdot s$)	3.61	2.84	9.21	2.85	1.60	9.27	18.99

In general, average τ_c and k_d values were greater for the upper bank position compared to the mid/lower bank positions. While τ_c values at the upper bank positions were greater signifying greater resistance to erosion than compared to the lower bank positions, the k_d values were also greater signifying greater erosion rates once the high flow stage reaches the upper bank. Differences in erodibility properties between the upper and lower bank position may be due to the upper bank soils being less cohesive than the lower bank soils, and subjected more to subaerial processes.

Stream Bank Retreat

By channel morphology/vegetation class, erosion pin data ranged between 0.91 and4.57 cm for straight channels with bank vegetation, 2.13 and 14.63 cm for straight channels without bank vegetation, 1.52 and 8.53 cm for curved channel outside bend with vegetation, and 17.37 and 23.77 cm for curved channel outside bend with vegetation (Table 5). Retreat estimates were generally less when vegetation was on the banks. As expected, retreat estimates were greatest on the outside bend of a curved channel without vegetation. Beeson and Doyle (1995) examined channel bends with and without vegetation and found that bends without vegetation had a 3000% potential of significant bank erosion compared to vegetated bends. To note at some locations, erosion pins were missing, thus at those sites retreat was approximated as 46 cm, the length of the installed rebar. It appears in general, more fluvial erosion occurred at lower-bank pin sites compared to the upper and middle bank pin sites. This observation is most likley due to greater frequency and longer durations of stream flows affecting the lower pin sites.

Table 5. Bank retreat average measurements for channel morphology/vegetation category and bank vertical position. Channel class (1 = straight channel with bank vegetation, 2 = straight channel with no bank vegetation, 3 = outside bend with bank vegetation, and 4= outside bend with no bank vegetation). Negative retreat indicates erosion.

Channel Class	Pin Position	No. of Pins	Avg. retreat (cm)	% of Pins not changing	% of Pins changing	% of Pins showing deposition	% of Pins showing erosion
Class 1	Upper	15	-2.74	6.7	93.3	21.4	71.9
	Mid	12	-0.91	8.3	91.7	9.1	82.6
	Low	17	-4.57	0.0	100.0	23.5	76.5
Class 2	Upper	13	-2.44	0.0	100.0	38.5	61.5
	Mid	9	-2.13	0.0	100.0	22.2	77.8
	Low	7	-14.63	0.0	100.0	42.9	57.1
Class 3	Upper	10	-1.52	0.0	100.0	20.0	80.0
	Mid	14	-5.18	21.4	78.6	9.09	69.5
	Low	12	-8.53	0.0	100.0	0.0	100.0
Class 4	Upper	4	-17.98	25.0	75.0	0.0	75.0
	Mid	6	-17.37	33.3	66.7	25.0	41.7
	Low	8	-23.77	0.0	100.0	12.5	87.5

At a few pin lower locations, deposition occurred apparently due to sediment from mass failure vertically above on the bank. The observed deposition material was compostead of loose soil. This soil will not be permanent and eventually be washed away. Deposition at erosion pins have been observed by others (Bradbury et al. 1995; Couper et al. 2002; Harden et al. 2009). In a few instances the deposition was enough to cover the erosion pin and it was marked as buried, and the amount of deposition was determined by using the prior retreat measurement. This method of measuring buried pin deposition is consistent with other studies, such as by Palmer et al. (2014). Buried pins at the end of the study period were not used to compute an α coefficient.

Pin Sites: Shear Stress Magnitudes and Durations

Flows during the 2019-2020 study period exhibited regular annual patterns for this region with the lowest discharges occurring during the fall, and high-flow discharges occurring in February and during the spring. Flow data during the study period for the three USGS gaging stations ranged between 0.011 and 22.654 m^3/s at Stock Creek, 0.198 and 198.218 m^3/s at Bullrun Creek, and 0.425 and 113.267 m^3/s at Beaver Creek. Development of the regression equations to estimate flow time series at the different study sites from the USGS StreamStats data are summarized in Condon (2020). Site stream discharges ranged from 0.011 m^3/s to 198.218 m^3/s.

Using HEC-RAS, models were created for each study site to determine the discharges (Q) in which fluvial erosion may be occurring (Condon 2020). Figure 2 illustrates the flow stages for the three pin positions vertically placed on a stream bank site. Flow stage 1 (Q1) occurred above the lower (L) pin; flow stage 2 (Q2) occurred above the mid (M) pin; and flow stage 3 (Q3) occurred above the upper (U) pin and may be termed bankfull. Values for Q and τ as shown in Figure 2, along with the time pins were exposed to potentially erosive flow were obtained from each site's HEC-RAS model (Table 6). Model cross-section and water surface elevations were inspected for multiple discharges. Manning n values used in HEC-RAS were 0.2 and 0.4 for the channel bed and the banks. respectively. As shown in Table 6, average shear stresses at the pins for Q1, Q2, and Q3 were computed as: $\tau_{(L)}$, $\tau_{(M)}$, and $\tau_{(U)}$, respectively (Table 3).

Table 6. Stream discharges, average applied shear stress, and durations for each study site and vertical pin position derived from flow time series and site HEC-RAS models.

Flow Stage	**Low Pins**				**Mid Pins**				**Upper Pins**			
Flow Variable / Study Site	**Q1 (m^3/s)**	Flow Event Totals	Total Time (hr)	**$\tau_{(L)}$ (Pa)**	**Q2 (m^3/s)**	Flow Event Totals	Total Time (hr)	**$\tau_{(M)}$ (Pa)**	**Q3 (m^3/s)**	Flow Event Totals	Total Time (hr)	**$\tau_{(U)}$ (Pa)**
North Bullrun Cr.	0.708	30	2334		2.831	16	421		8.495	8	146	
South Bullrun Cr.	1.133	35	2414		3.256	18	650		8.495	11	216	
Bullrun Cr., Maynard-ville	0.991	32	4335		4.246	25	1076		11.327	14	284	
Stock Creek	0.425	39	3819		2.831	44	778		11.327	14	106	
Beaver Cr., Clayton	0.425	31	6474		1.416	31	2892		9.911	9	268	
Beaver Cr., Halls	0.227	38	7131		0.850	35	3277		2.124	20	1032	
Hines Branch	0.142	40	3186		0.566	12	510		2.124	1	32	
Beaver Cr., Cox	0.283	34	7179		1.133	35	2203		3.483	12	524	
Beaver Cr., Cox (*)	0.283	21	5646		1.133	31	2048		3.483	11	488	

Note: (*) pins installed in June 2019.

Discharges and flow event totals and durations per site varied primarily based on drainage area size, the larger the drainage area the greater the discharges per stage, and the number of events with pins exposed to erosive flows (Table 6). Flow event totals and duration were greater at the low pin position than the upper pin positions. Average applied shear stresses were also greater at the low pin position than the upper pin positions. The stresses ranged from 2.946 to 55.258 Pa for the lower pin, 2.6173 to 57.195 Pa for the mid pins, and 3.561 to 45.165 Pa for the upper pins. These average estimates were simplified based on three flow stages applying Bagnold (1960) linear derivation of instream shear stresses from the water surface ($\tau = 0$) to the channel bed (τ = maximum). These average stresses per study site and pin position were used to compute α coefficients in the modified excess shear stress equation.

Modified Excess Shear Stress Equation

The modified shear stress equation, rearranging for computation of the α coefficient becomes: $\alpha =(\varepsilon_r/k_d,+ \tau_c)/\tau$. All parameters were field measured or computed through HEC-RAS modeling, and summarized for the four channel morphology/vegetation classes (Figure 3, Table 7). Only values where $\tau > \tau_c$ was used to estimate an α coefficient. In cases were deposition or erosion did not occur an α coefficient was not calculated since the equation is only meant to predict erosion. Per channel morphology/vegetation class, α coefficients averaged 0.3467, 0.2677, 0.2504, and 0.3100 for straight channels with and without vegetation and outside bend to curved channels with and without vegetation, respectively. All α coefficients were less than one indicating that the excess shear stress equation tends to overpredict fluvial erosion rates, thus annual estimated for bank retreat. Coefficients were greater for the outside bend of curved channels compared to straight channels indicating greater erosion rates for curved channels. This result would be expected from geomorphic processes for meandering channels (Knighton 1998). In addition, on

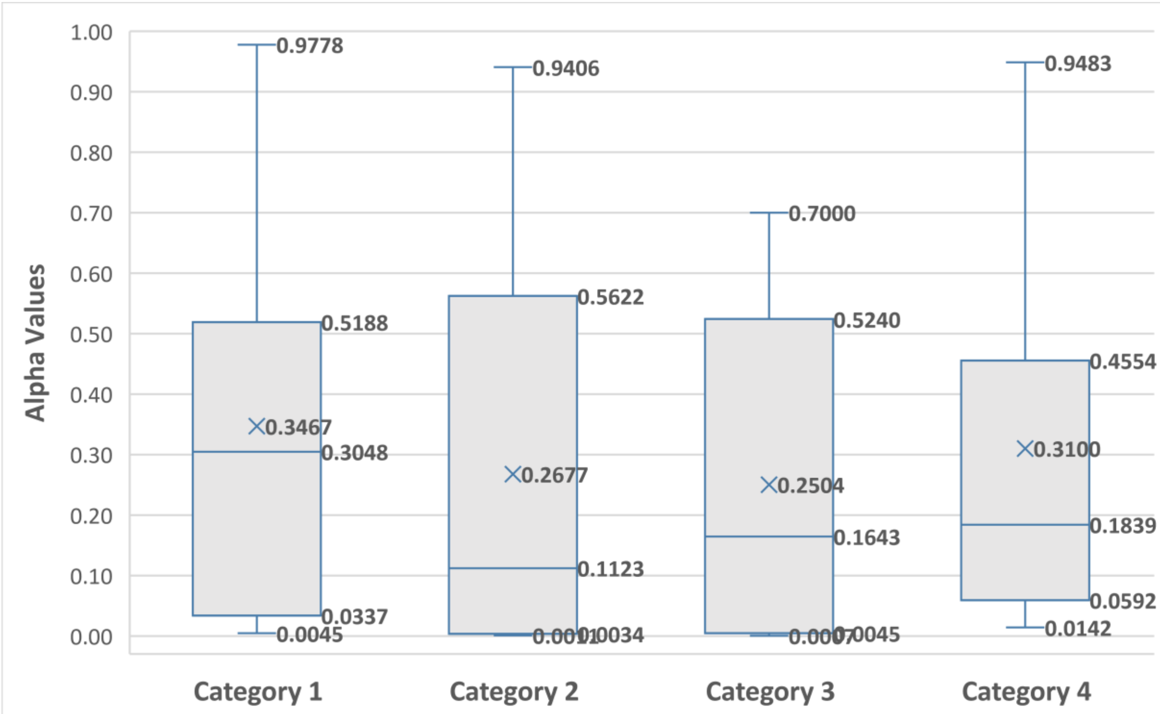

Figure 3. Box plots of α coefficients in the modified excessive shear stress equation for the four channel morphology/vegetation classes. Channel classes (categories): 1 = straight channel with bank vegetation; 2 = straight channel with no bank vegetation; 3 = outside bend with bank vegetation; and 4= outside bend with no bank vegetation.

Table 7. Summary of coefficients in the modified excessive shear stress equation for the four channel morphology/vegetation classes.

Channel Morphology/ Vegetation Class	**Straight with bank vegetation**	**Straight with no bank vegetation**	**Curved with bank vegetation**	**Curved with no bank vegetation**
Class Number	**1**	**2**	**3**	**4**
Number of values	31	18	24	12
Average	0.3467	0.2677	0.2504	0.3100
Min	0.0045	0.0011	0.0007	0.0142
Max	0.9778	0.9406	0.7000	0.9483
Standard Deviation	0.3176	0.3173	0.2506	0.3189
Variance	0.1090	0.0773	0.0609	0.1045

average straight and curved channels without vegetation were observed with a smaller α coefficient compared to the same channel class with vegetation indicating greater fluvial erosion rate for unprotected banks. Much literature has been published on the protective role of bank vegetation from excessive erosion (Beeson and Doyle 1995; Curran and Hession 2013; Hopkinson and Wynn-Thompson 2016; Peacher et al. 2018). Different properties of the vegetative plant types used will determine if stabilization will occur. It has been found that plant roots will remove water which strengthens the banks (Simon and Collison 2002). Wynn and

Mostaghimi (2006) found that thick non-woody vegetation can reduce bank erosion by reducing the water content of the soil and keeping it from freezing. This is important to manage in the winter months when bank erosion is greatest (Wolman 1959; Willett et al. 2012).

Overall, α coefficients varied greatly between 0.0005 and 0.7299 (Table 7). Box plots per the four channel classes in Figure 3 illustrate the wide range of coefficients. Because of the wide range, data were log transformed and class groups compared using unequal variance t-tests. Significant differences were observed between straight channels vegetated and no vegetated ($p = 0.038$) and non-vegetated straight and curved channels ($p = 0.034$). Statistical analyses for curved channels vegetated and non-vegetated resulted in $p = 0.062$, and vegetated straight and curved channels results in $p = 0.071$).

Conclusions

The four different channel morphology/vegetation classes were chosen to determine their effects on fluvial erosion rates as estimated by the excess shear stress equation. Annual bank retreat for straight channel with vegetation ranged from -0.91 to -4.57 cm, straight channels without vegetation ranged from -2.13 to -14.63 cm, outside bends of curved channels with vegetation ranged from -1.52 to -8.53 cm, and outside bends of curved channels without vegetation ranged from -17.37 to -23.77 cm. Bank retreat rates were substantially reduced with vegetation. Vegetation increases hydraulic resistance, thus reducing applied τ at the bank. Outside bends of curved channels without vegetation exhibited the greatest annual retreats. This result supports the need to modify the excess shear stress equation with an α coefficient to amount for channel characteristics (Langendoen and Simon 2008, 2009; Daly et al. 2015b).

Results found that erosion rates using the excess shear stress equation overpredicted annual bank retreat, and provided evidence that an α coefficient is needed modifying the equation as follows: equation $\varepsilon_r = k_d\,(\alpha \cdot \tau - \tau_c)$. Values for the α coefficient were computed as less than one reducing the erosion rates if the excess shear stress equation is used to estimate annual bank retreat. Per channel morphology/vegetation class, α coefficients averaged 0.3467, 0.2677, 0.2504, and 0.3100 for straight channels with and without vegetation and outside bend to curved channels with and without vegetation, respectively.

The α coefficients computed for each channel class were highly varied and likely due to multiple factors. Some factors may include the variability associated with measuring k_d, and τ_c (Mahalder et al. 2018); heterogeneity of bank erodibility properties (Daly et al. 2015a); density of bank roots and bank vegetation composition (Wynn 2004; Curran and Hession 2013); and issues with measuring pin erosion (Meyers et al. 2019). The α coefficient computation was dependent on the Manning n values used in the HEC-RAS models to estimate an average τ per three flow stages. This study used standard, constant Manning's n values for channel bed and banks. These values were not calibrated with continuous stage measurements at each site die to limited resources for stage recorders. Future studies can improve estimates for α coefficients for these channel morphology/vegetation classes and other classes with more specific criteria to qualify the class, and on-site flow monitoring and HEC-RAS model calibrations.

References

Addul-Kadir, M.A., and Ariffin, J. 2012. "Advances on bank erosion studies: A review," ASM Science Journal 6(2): 128-137.

Addy, S., and Wilkinson, M. 2019. " Representing natural and artificial in-channel large wood in numerical hydraulic and hydrological models," Water 6(6): 1-20, 10.1002/wat2.1389.

Al-Madhhachi, A.T., Hanson, G.J., Fox, G.A., Tyagi, A.K., and Bulut, R. 2013. "Measuring soil erodibility using a laboratory 'mini' JET," Transactions of the ASABE 56(3): 901–910.

Allmanová, Z., Vlčková, M., Jankovskỳ, M., Jakubis, M., and Allman. M. 2019. “Bank erosion of the Tŕstie Stream: BANCS model predictions versus real bank erosion,” Journal of Hydrology and Hydromechanics 67(2): 121–128.

Anim, D.O., Fletcher, T.D., Vietz, G.J., Pasternack, G.B., and Burns, M.J. 2018. “Effect of urbanization on stream hydraulics: urbanization and stream hydraulics,” River Research and Applications 34 (7): 661–674.

Bagnold, R.A. 1960. Sediment Discharge and Stream Power: A Preliminary Announcement. Geological Survey Circular 421, US Geological Survey, Washington D.C.

Beeson, C.E., and Doyle, P.F. 1995. “Comparison of bank erosion at vegetated and non-vegetated channel bends,” Journal of the American Water Resources Association 31(6): 983–990.

Bledsoe, B.P., and Watson, C.C. 2001. “Effects of urbanization on channel instability,” Journal of the American Water Resources Association 37(2): 255–270.

Booth, D.B., and Fishenich, C.J. 2015. A Channel Evolution Model to Guide Sustainable Urban Stream Restoration. “ Area, 10.1111/area.12180.

Bradbury, J., Cullen, P., Dixon, G., and Pemberton, M. 1995. “Monitoring and management of streambank erosion and natural revegetation on the Lower Gordon River, Tasmanian Wilderness World Heritage Area, Australia,” Environmental Management 19(2): 259–722.

Briaud, J.L., Ting, F.C.K., Chen, H.C., Cao, Y., Han, S.W., and Kwak. K.W. 2001. “Erosion function apparatus for scour rate predictions,” Journal of Geotechnical and Geoenvironmental Engineering 127(2): 105–113.

Chen, D., and Duan, J.G. 2005. “Modeling width adjustment in meandering channels. Journal of. Hydrology 321(1-4): 59-76.

Clark, L.A. and Wynn, T. M. “Methods for determining streambank critical shear stress and soil erodibility: implications for erosion rate predictions,” Trans. ASABE 50(1): 95–106.

Condon, J.C. 2020. Improving stream bank erosion estimates by adjusting the applied shear stress for different bank characteristics. MS Thesis, University of Tennessee, Knoxville.

Couper, P., Stott, T., and Maddock, I. 2002. “Insights into river bank erosion processes derived from analysis of negative erosion-pin recordings: observations from three recent UK studies.” Earth Surface Processes and Landforms 27(1): 59–79.

Curran, J.C., and Hession, W.C. 2013. Vegetative impacts on hydraulics and sediment processes across the fluvial system,” Journal of Hydrology 505-376. : 364

Daly, E.R., Fox, G.A., Al-Madhhachi, A.T., and Miller, R.B. 2013. “A scour depth approach for deriving erodibility parameters from jet erosion tests,” Trans. ASABE 56(6): 1343–1351.

Daly, E.R., Fox, G.A., Enlow, H.K., Storm, D.E., and Hunt, S.L. 2015a. Site-scale variability of streambank fluvial erodibility parameters as measured with a jet erosion test,” Hydrological Processes 29(26): 5451–5464.

Daly, E.R., Miller, R.B., and Fox, G.A. 2015b. “Modeling Streambank Erosion and Failure along Protected and Unprotected Composite Streambanks,” Adv. Water Resources 81: 114–127.

Davis, L. and Harden C.P. 2014. “Factors contributing to bank stability in channelized, alluvial streams,” River Research and. Applications 30(1): 71-80.

DeRobertis, A., Ryer, C.H., Veloza, A., and Brodeur, R.D. 2003. “Differential effects of turbidity on prey consumption of piscivorous and planktivorous fish,” Canadian Journal of Fisheries & Aquatic Sciences 60: 1517–1526.

Dietrich, W.E. 1987. “Mechanics of flow and sediment transport in river bends,” In River Channel Environment and Process, K. Richards (ed.). Blackwell Press: Oxford; 179–227.

Duan, J.G. 2005. “Analytical approach to calculate rate of bank erosion,” Journal of Hydraulic Engineering 131(11): 980-990.

Ferguson, R.I., Parsons, D.R., Lane, S.N., and Hardy, R.J. 2003. “Flow in meander bends with recirculation at the inner bank,” Water Resources Research 39(11): 1322.

Govenor, H., Krometis, L.A.H., and Hession, W.C. 2017. “Invertebrate-based water quality impairments and associated stressors identified through the US Clean Water Act. Environmental Management,” 60: 598–614.

Green, T.R., Beavis, S.G., Dietrich, C.R., and Jakeman, A.J. 1999. "Relating stream-bank erosion to in-stream transport of suspended sediment," Hydrological Processes 13(5): 777–787.
Hanson, G.J., and Cook, K.R. 2004. "Apparatus, test procedures, and analytical methods to measure soil erodibility in-situ," Appl. Eng. Agric. 20:455–462.
Hanson, G.J. 1990a. "Surface erodibility of earthen channels at high stresses (Part I) -open channel testing," Transactions of the ASAE 33(1):: 127–131.
Hanson, G.J. 1990b. "Surface erodibility of earthen channels at high stresses (Part II) -developing an in-situ testing device," Transactions of the ASAE 33(1): 132–137.
Hanson, G.J., and Simon, A. 2001. "Erodibility of cohesive streambeds in the loess area of the midwestern USA," Hydrological Processes 15(1): 23–38.
Harden, C.P., Foster, W., Morris, C., Chartrand, K.J., and Henry, E. 2009. "Rates and processes of streambank erosion in tributaries of the Little River, Tennessee." Physical Geography 30(1): 1-16.
Henley, W. E., Patterson, M. A., Neves, R. J., and Lemly, A.D. 2000. "Effects of sedimentation and turbidity on lotic food webs: A concise review for natural resources managers," *Reviews in Fisheries Science 8*(2): 125–139.
Hopkinson, L.C. and Wynn-Thompson, T.M. 2016. "Comparison of direct and indirect boundary shear stress measurements along vegetated streambanks," River Res.& Applications 32(8): 1755-1764.
Ismail, H., Xu, Y., and Liu, X. 2021. "Flow and scour around idealized porous engineered log jam structures," Journal of Hydraulic Engineering 147(1): 04020089-2.
Kean, J.W., and Smith, J.D. 2004. "Flow and boundary shear stress in channels with woody bank vegetation," In Water Science and Application, S.J. Bennett & A. Simon (eds.), 8: 237–252. American Geophysical Union, Washington, D. C.
Khanal, A., Fox, G.A., and Al-Madhhachi, A.T. 2016. "Variability of erodibility earameters from laboratory mini jet erosion tests," Journal of Hydrologic Engineering 21(10): 04016030.
Klavon, K., Fox, G.A., Guertault, L. Langendoen, E., Enlow, H., Miller, R., and Khanal. A. 2017. "Evaluating a process-based model for use in streambank stabilization: insights on the Bank Stability and Toe Erosion Model (BSTEM," Earth Surf. Proc.& Landforms 42(1): 191–213.
Knighton, D. 1998. Fluvial Forms and Processes: A New Perspective, 2nd Ed. Hodder Arnold Publ.
Kronvang, B., Andersen, H.E., and Larsen, S.E. 2013. "Importance of bank erosion for sediment input, storage and export at the catchment scale," *J Soils Sediments* **13**, 230–241.
Langendoen, E.J. 2000. Conservational Channel Evolution and Pollutant Transport System (CONCEPTS). User's Manual, USDA National Sedimentation Laboratory, Oxford, MS.
Langendoen, E.J., and Simon, A. 2018. "Modeling the evolution of incised streams. II: Streambank erosion," Journal of Hydraulic Engineering 134(7): 905–915.
Langendoen, E.J., and Simon, A. 2009. "Closure to 'Modeling the Evolution of Incised Streams. II: Streambank erosion," Journal of Hydraulic Engineering 135(12): 1107–1108.
Lawler, D.M. 1993. "The measurement of river bank erosion and lateral channel change: A review,: Earth Surf. Proc.& Landforms 18(9): 777-821.
Lawler, DM. 2008. "Advances in the continuous monitoring of erosion and deposition dynamics: Developments and applications of the new PEEP-3T system," Geomorphology 93(1-2): 17-39.
Mahalder, B. Schwartz, J.S., Palomino, A.M., and Zirkle, J. 2018. Estimating erodibility parameters for streambanks with cohesive soils using the mini jet test device: a comparison of field and computational methods," Water: 304. https://doi.org/10.3390/w10030304.
Mahalder, B., Schwartz, J.S., Palomino, A.M., and Zirkle, J. 2017. Relationships between streambank erosion and physical-geochemical properties of cohesive soils among physiographic regions of Tennessee, USA. Earth Surf. Proc.& Landforms 43: 401-416.
Mahalder, B. Schwartz J.S. Thompson-Wynn, T.M., Palomino, A.M and Zirkle, J. 2022. "Comparison of erodibility parameters for cohesive streambank soils between an in-situ jet test device and laboratory conduit flume," Journal of Hydraulic Engineering 148(1): 04021055-2.
Manner, R.B., Doyle, M.W., and Small, M.J. 2007. "Structure and hydraulics of natural woody debris jams," Water Resources Research 43, W06432.

Midgley, T.L., Fox, G.A., and Heeren, D.M. 2012. “Evaluation of the Bank Stability and Toe Erosion Model (BSTEM) for Predicting Lateral Retreat on Composite Streambanks,” Geomorphology 145–146: 107–114.
Mostafa, T.M.S., Imran, J., Chaudhry, M.H., and Khan, I.B.. 2008. “Erosion resistance of cohesive soils,” Journal of Hydraulic Research 46(6): 777–787.
Myers, D.T., Rediske, R.R., and McNair, J.N. 2019. “Measuring streambank erosion: a aomparison of erosion pins, total station, and terrestrial laser scanner,” *Water 11*(9), 1846.
Newcombe, C.P., and Jensen, J.O.T. 1996. “Channel suspended sediment and fisheries: a synthesis for quantitative assessment of risk and impact,” North American Journal of Fisheries Management 16(4): 693–719.
Palmer, J.A., Schilling, K.E., Isenhart, T.M., Schultz, R.C., and Tomer, M.D. 2014. “Streambank erosion rates and loads within a single watershed: bridging the gap between temporal and spatial scales,” Geomorphology 209: 66–78.
Peacher, R.D., Lerch, R.N., Schultz, R.C., Willett, C.D., and Isenhart, T.M. 2018. “Factors controlling streambank erosion and phosphorus loss in claypan watersheds,” Journal of Soil and Water Conservation 73(2): 189–199.
Pope, I.C., and Odhiambo, B. 2013. “Soil erosion and sediment fluxes analysis: A watershed study of the Ni Reservoir, Spotsylvania County, VA, USA. Environmental Monitoring and Assessment 186(3): 1719-1733.
Rosgen, D.L. 1996. Applied River Morphology. Wildlands Hydrology Publ. Colorado.
Rosgen, D.L. 2006. Watershed Assessment of River Stability and Sediment Supply. Altona, Manitoba, Canada: Friesens Printing.
Saadon, A., Abdullah, J., Muhammad, N.S., Ariffin, J., and Julien, P.Y. 2021. “Predictive models for the estimation of riverbank erosion rates,” Catena 196: 104917.
Schwartz, J.S., Dahle, M., and Robinson, R.B. 2008. “Concentration-frequency-duration curves for stream turbidity: possibilities for use assessing biological impairment,” Journal of the American Water Resources Association 44(4): 879-886.
Schwartz, J.S., Simon, A., and Klimetz, L. 2011. “Use of fish functional traits to associate in-stream suspended sediment transport metrics with biological impairment,” Environmental Monitoring and Assessment 179: 347–369.
Schilling, K.E., Isenhart, T.M., Palmer, J.A., Wolter, C.F., and Spooner, J. 2011. “Impacts of land-cover change on suspended sediment transport in two agricultural watersheds,” Journal of the American Water Resources Association 47(4): 672–686.
Shields, F.D., Knight, S.S., and Cooper, C.M. 1995. “Rehabilitation of watersheds with incising channels,” Water Resources Bulletin 31(6): 971-982.
Simon, A. 1995. “Adjustment and recovery of unstable alluvial channels: Identification and approaches for engineering management,” Earth Surf. Processes & Landforms 20: 611-628.
Simon, A., and Downs, P.W. 1995. “An interdisciplinary approach to evaluation of potential instability in alluvial channels,” Geomorphology 12: 215–232.
Simon, A., and Darby, S.E. 1999. “The nature and significance of incised river channels,” in S.E. Darby, and A. Simon (Eds.), Incised Rivers Channels: Processes, Forms, Engineering, and Management, p. 3–18. UK: John Wiley and Sons.
Simon, A., Curini, A., Darby, S.E., and Langendoen, E.J. 2000. “Bank and near-bank processes in an incised channel,” Geomorphology 35: 193–217.
Simon, A., and Rinaldi, M. 2000. “Channel instability in the loess area of the Midwestern United States,” Journal of the American Water Resources Association 36(1): 138–150.
Simon, A, and Collision, A.J.C. 2002. “Quantifying the mechanical and hydrologic effects of riparian vegetation on streambank stability,” Earth Surf. Proc. & Landforms 27: 527-546.
Simon, A. and Thomas, R.E. 2002. “Processes and forms of an unstable alluvial system with resistant, cohesive streambanks,” Earth Surf. Processes & Landforms 27: 699-718.

Simon, A., Heins, A., and Dickerson, W. 2004.”Suspended sediment transport rates at the 1.5-year recurrence interval for ecoregions of the United States: Transport conditions at the bankfull and effective discharge?” Geomorphology 58: 243–262.
Simon, A., and Klimetz, L. 2008. “Magnitude, frequency, and duration relations for suspended sediment in stable (“reference”) southeastern streams,” Journal of the American Water Resources Association 44(5): 1270–1283.
Simon, A., R. E. Thomas, and L. Klimetz. 2010. “Comparison and experiences with field techniques to measure critical shear stress and erodibility of cohesive deposits,” In Proc. 2nd Joint Federal Interagency Conference, ASCE, Reston, Virginia
Sturm, T.W. 2021. Open Channel Hydraulics, 3rd edition. McGraw-Hill Education.
Smith, D.J., Wynn-Thompson, T.M., Williams, M.A., and Seiler, J.R. 2021. Do roots bind soil? Comparing the physical and biological role of plant roots in fluvial streambank erosion: A mini-JET study,” Geomorphology 375: 107523.
Termini, D. 2016. Experimental analysis of the effect of vegetation on flow and bed shear stress distribution in high-curvature bends,” Geomorphology 274: 1-10.
Thorne, C.R., and Tovey, N.K. 1981. “Stability of composite river banks,” Earth Surface Processes and Landforms (5): 469–484.
USEPA. 2000. National Water Quality Inventory to Congress. EPA-841-R-02-001. Office of Water, US Environmental Protection Agency, Washington D.C.
USEPA. 2006. Framework for developing Suspended and Bedded Sediments (SABS) water quality criteria, EPA-822-R-06–001. Office of Water, Office of Research and Development. US Environmental Protection Agency, Washington D.C.
Violin, C.R., Cada, P., Sudduth, E.B., Hassett, B.A., Penrose, D.L., and Emily S. Bernhardt, E.S. 2011. “Effects of Urbanization and Urban Stream Restoration on the Physical and Biological Structure of Stream Ecosystems,” Ecological Applications 21(6): 1932–1949.
Wan, C.F., and Fell, R. 2004. “Investigation of rate of erosion of soils in embankment dams,” Journal of Geotechnical and Geoenvironmental Engineering 130(4): 373–380.
Waters, T.F. 1995. Sediment in streams: Sources, Biological Effects, and Control. American Fisheries Society, Bethesda, MD.
Willett, C.D., Lerch, R.N., Schultz, R.C., Berges, S.A., Peacher, R.D., and Isenhart, T.M. 2012. “Streambank erosion in two watersheds of the Central Claypan Region of Missouri, United States.” Journal of Soil and Water Conservation 67(4): 249–263.
Wolman, M.G. 1959. “Factors influencing erosion of a cohesive river bank,” American Journal of Science 257(3): 204–216.
Wood, P.J., and Armitage, P.D. 1997. “Biological effects of fine sediment in the lotic environment, “ Environmental Management, 28, 255–266.
Wynn, T.M. 2004. The Effects of Vegetation on Stream Bank Erosion. PhD dissertation, Virginia Polytechnic Institute & State University, Blacksburg, Va.
Wynn, T.M., and Mostaghimi, S. 2006. “The effects of vegetation and soil type on streambank erosion, southwestern Virginia, USA,” Journal of the Amer. Water Resources Association 42(1): 69–82.
Yu, M-H, Wei, H., and Wu, S. 2015. “Experimental study on the bank erosion and interaction with near-bank bed evolution due to fluvial hydraulic force,” International Journal of Sediment Research 30, 10.1016/S1001-6279(15)60009-9.